

Dalton Transactions

Accepted Manuscript



This is an *Accepted Manuscript*, which has been through the Royal Society of Chemistry peer review process and has been accepted for publication.

Accepted Manuscripts are published online shortly after acceptance, before technical editing, formatting and proof reading. Using this free service, authors can make their results available to the community, in citable form, before we publish the edited article. We will replace this *Accepted Manuscript* with the edited and formatted *Advance Article* as soon as it is available.

You can find more information about *Accepted Manuscripts* in the [Information for Authors](#).

Please note that technical editing may introduce minor changes to the text and/or graphics, which may alter content. The journal's standard [Terms & Conditions](#) and the [Ethical guidelines](#) still apply. In no event shall the Royal Society of Chemistry be held responsible for any errors or omissions in this *Accepted Manuscript* or any consequences arising from the use of any information it contains.

Cite this: DOI: 10.1039/c0xx00000x

www.rsc.org/xxxxxx

ARTICLE

Varied forms of lamellar $[\text{Sn}_3\text{Se}_7]_n^{2n-}$ anion: the competitive and synergistic structural directing effects of metal-amine complex and imidazolium cations

Cheng-Feng Du,^{a,b} Jian-Rong Li,^{*a} Mei-Ling Feng,^a Guo-Dong Zou,^c Nan-Nan Shen^{a,b} and Xiao-Ying Huang^a

Received (in XXX, XXX) Xth XXXXXXXXXX 20XX, Accepted Xth XXXXXXXXXX 20XX

DOI: 10.1039/b000000x

Presented is the syntheses, characterizations and properties of a series of selenidostannate compounds directed by metal-amine complex (MAC) cations and/or $[\text{Bmmim}]^+$ (Bmmim = 1-butyl-2,3-dimethyl-imidazolium). A mixture of the ionic liquid (IL) (Bmmim)Cl and amines such as ethylenediamine (en) and diethylenetriamine (dien) in various ratios was used to ionothermally/solvothermally prepare four selenidostannates, namely $[\text{Mn}(\text{en})_3][\text{Sn}_3\text{Se}_7]$ (**1**), $[\text{Mn}(\text{dien})_2][\text{Sn}_3\text{Se}_7 \cdot \text{H}_2\text{O}]$ (**2**), $(\text{Bmmim})_3[\text{Mn}(\text{en})_3]_2[\text{Sn}_9\text{Se}_{21}]\text{Cl}$ (**3**) and $(\text{Bmmim})_6[\text{Mn}(\text{dien})_2]_2\text{Sn}_{15}\text{Se}_{35}$ (**4**). Single-crystal X-ray diffraction analyses revealed that the compounds feature of lamellar anionic $[\text{Sn}_3\text{Se}_7]_n^{2n-}$ structures. The $[\text{Sn}_3\text{Se}_7]_n^{2n-}$ layers in **1–4** all possess a $\{6^3\}$ net considering the $[\text{Sn}_3\text{Se}_{10}]$ semi-cube unit as a 3-connected node, however, there exist diverse multi-membered rings. In compounds **1** and **2**, all the $[\text{Sn}_3\text{Se}_{10}]$ units are 3-connected nodes interlink to each other *via* edge-sharing two Se atoms to produce six-membered rings. While in compound **3** the insertion of two $[\text{Sn}_3\text{Se}_9]$ units into the six-membered ring results in a novel eight-membered heart-shaped ring, which has never been observed before in the family of chalcogenidostannates. More interestingly, the $[\text{Sn}_3\text{Se}_7]_n^{2n-}$ layer in compound **4** consists of mixed six- and eight-membered rings. The phase isolation is strongly dependent on the ratio of IL and MAC in the syntheses, that is, **1** and **2** were obtained with the IL:MAC ratios less than 3:1 and 4:1, respectively, while **3** and **4** were obtained when the ratios were increased to 4:1 and 5:1, respectively. The structural variation from **1–4** clearly indicates the competitive and synergistic effects between MAC and cation of IL on the formation of lamellar selenidostannates. The synthetic approach *via* varying the ratio of MAC and IL cation as solvent and structural directing agents shall be attractive in the synthesis of novel chalcogenidometallates.

Cite this: DOI: 10.1039/c0xx00000x

www.rsc.org/xxxxxx

ARTICLE

Introduction

The chalcogenidometallate compounds have continuously been of great academic and industrial interest, not only for their fascinating architectures and topologies but also for their unique physical properties and potential applications in areas such as fast-ion conductivity, photocatalysis, sensing, and ion-exchange.¹⁻⁶ In the synthesis of chalcogenidometallates, the organic amines or alkali metal cations were typically chosen as template or structural directing agents (SDA).^{3, 7-13} Recently, metal-amine complexes (MACs) have also been found to be an effective SDA in directing chalcogenidometallates.¹⁴⁻¹⁸ On the other hand, the excellent solvating properties and structural directing effects of ionic liquids (ILs) have made them be a promising media in inorganic synthesis.¹⁹⁻²³ Especially, the specific ionic environment of ILs would aid the formation of novel compounds that are inaccessible in traditional molecular solvents. For instance, the research from our and Dehnen's groups showed that the combination of ILs and organic amine as auxiliary solvent was an efficient system for the fabrication of selenidostannates, in which the organic amines and cations of ILs might co-induce specific structures.^{24, 25} The similar phenomena have been observed in the ionothermal syntheses of zeolites;²⁶⁻²⁹ for example, a new open-framework aluminophosphate with unique Al/P ratio was synthesized by using amine and ILs as the co-templates.^{26, 29} Thus we realize that the synthesis in ILs with different SDAs would produce highly novel structures due to the chemical and compositional flexibility of SDAs. However, until now there is still no report on the ionothermal synthesis of chalcogenidometallates that simultaneously contains MACs and IL cations.

The Sn^{4+} ion tends to adopt four or five coordination geometries with chalcogen ions, which often undergo a variety of self-condensation to form $[\text{Sn}_2\text{Q}_6]$ ($\text{Q} = \text{S}, \text{Se}$),^{8, 9, 30, 31} $[\text{Sn}_3\text{Q}_{10}]$,^{7, 10, 11, 32-51} and $[\text{Sn}_4\text{Q}_{10}]$.^{31, 41, 52} By using these binary aggregates as secondary building units (SBUs), plenty of chalcogenidostannates with varied structural dimensionalities have been obtained. Among them, it is interesting that the $[\text{Sn}_3\text{Q}_{10}]$ units as SBUs can interlink to each other via sharing two $\mu_2\text{-Q}$ bridging atoms resulting in distinct structures of $[\text{Sn}_3\text{Q}_7]_n^{2n-}$ ranging from single-chain,^{40, 47, 53} double-chain,^{47, 48} layer^{11, 36, 40, 42, 43, 45, 47-49, 51} to that coexisting single-chain and layer.^{41, 50} Particularly, the family of two-dimensional (2D) chalcogenidostannates displays a rich diversity of lamellar $[\text{Sn}_3\text{Q}_7]_n^{2n-}$ ($\text{Q} = \text{S}, \text{Se}$) anion configurations in the presence of different SDAs and/or guest molecules (Fig. S1, ESI†).^{10, 32, 38, 41, 43} A very recent report was the formation of polymer/chalcogenide composite of $[\text{DBNH}]_2[\text{Sn}_3\text{Se}_7]\cdot\text{PEG}$ (PEG = polyethyleneglycol), demonstrating the remarkable framework flexibility of $[\text{Sn}_3\text{Q}_7]_n^{2n-}$.

Herein, we chose the selenidostannates as a model system to study the synergistic structural directing effect of MACs and

cation of ILs in the preparation of crystalline chalcogenidometallates. We report on the syntheses, structures and physical properties of four different selenidostannates, namely, $[\text{Mn}(\text{en})_3]\text{Sn}_3\text{Se}_7$ (**1**, en = ethylenediamine), $[\text{Mn}(\text{dien})_2]\text{Sn}_3\text{Se}_7\cdot\text{H}_2\text{O}$ (**2**, dien = diethylenetriamine), $(\text{Bmmim})_3[\text{Mn}(\text{en})_3]_2[\text{Sn}_9\text{Se}_{21}]\text{Cl}$ (**3**, Bmmim = 1-butyl-2,3-dimethyl-imidazolium) and $(\text{Bmmim})_6[\text{Mn}(\text{dien})_2]_2[\text{Sn}_{15}\text{Se}_{35}]$ (**4**). The structures feature lamellar anions of $[\text{Sn}_3\text{Se}_7]_n^{2n-}$ with different multi-membered rings. As shown in Fig. 1, the $[\text{Sn}_3\text{Se}_{10}]$ units are edge-shared to form six-membered elliptic rings in **1** and **2**, while insertion of two $[\text{Sn}_3\text{Se}_9]$ units into the six-membered ring leads to the eight-membered heart-shaped rings in **3**, and mixed six- and eight-membered rings in **4**, respectively. To the best of our knowledge, such novel eight-membered heart-shaped ring of $[\text{Sn}_3\text{Se}_7]_n^{2n-}$ has never been reported before. In combination with single-crystal X-ray diffraction, elemental analysis (EA) and thermogravimetric analysis (TGA), we demonstrate that both the MACs and IL cations are located in **3** and **4** simultaneously. The structural directing effect of MAC and imidazolium cation was studied in detail, revealing that the phase isolation was strongly dependent on the ratio of IL to MAC in the syntheses. The structural variation from **1** to **4** clearly indicates the competitive and synergistic effects between MAC and imidazolium cation on the formation of lamellar selenidostannates.

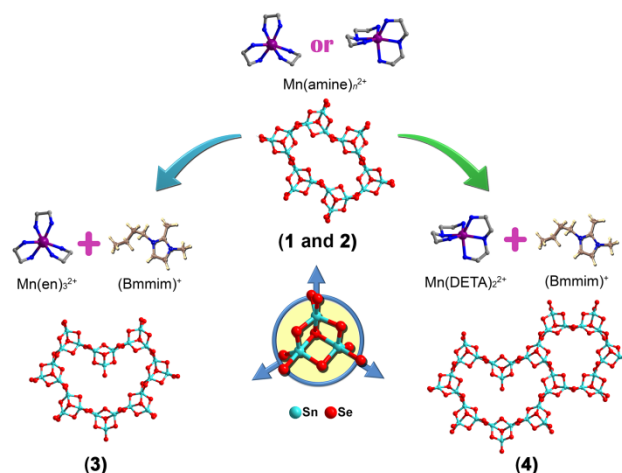


Fig. 1 Three different ring-based lamellar $[\text{Sn}_3\text{Se}_7]_n^{2n-}$ structures form in the presence of different structural directing cations.

Experimental section

Materials and physical measurements

Tin (99.5%) powder and $\text{MnCl}_2\cdot 4\text{H}_2\text{O}$ (AR) were purchased from Sinopharm Chemical Reagent, selenium (analytical grade) powder was purchased from Tianjin Yingda Rare Chemical Reagent, $(\text{Bmmim})\text{Cl}$ (99%) was purchased from Lanzhou Institute of Chemical Physics, and en (99%) and dien (99%) were

purchased from Aladdin and Adamas, respectively. All the chemicals were used without further purification. Powder X-ray diffraction (PXRD) patterns were recorded on a Rigaku Miniflex-II diffractometer by using CuK α radiation. Elemental analysis was performed on a German Elementary Vario EL III instrument. Thermogravimetric analysis (TGA) was carried out on a NETZSCH STA 449F3 unit at a heating rate of 10 K min⁻¹ under a N₂ atmosphere. Optical diffuse reflectance spectra were recorded at room temperature on a Shimadzu UV-2550 UV-Vis spectrophotometer, with a BaSO₄ plate as a standard (100% reflectance). The absorption data were calculated from reflectance spectra by using the Kubelka-Munk function $F(R_{\infty})$: $F(R_{\infty}) = (1 - R_{\infty})^2 / 2R_{\infty}$, where R_{∞} is the reflection coefficient of the sample.^{54, 55}

15 Syntheses of [Mn(en)₃][Sn₃Se₇] (1), [Mn(dien)₂][Sn₃Se₇·H₂O] (2), (Bmmim)₃[Mn(en)₃]₂[Sn₉Se₂₁]Cl (3) and (Bmmim)₆[Mn(dien)₂]₂[Sn₁₅Se₃₅] (4)

A mixture of Sn (0.119 g, 1 mmol), Se (0.198 g, 2.5 mmol), MnCl₂·4H₂O (0.099 g, 0.5 mmol) with 0.570 g [Bmmim]Cl (3 mmol) and 0.480 g en (8 mmol) was sealed in a 20 mL Teflon-lined stainless-steel autoclave at 160 °C for 5 days, followed by slowly cooling to room temperature under a cooling rate of ~5.4 K min⁻¹. The product was washed with DMF and ethanol for several times. Red crystals of **1** were obtained by manually selection (yield: 0.230 g, 60.2% based on Sn). Elemental analysis, calcd. (%) for C₆H₂₄MnN₆Se₇Sn₃: C 6.29, H 2.10, N 7.34; found: C 6.23, H 2.06, N 7.01.

When en was replaced by dien (0.520 g, 5 mmol) in the similar conditions, red block crystals of compound **2** could be obtained (yield: 0.180 g, 45.3% based on Sn). Elemental analysis, calcd. (%) for C₈H₂₈MnN₆OSe₇Sn₃: C 8.08, H 2.36, N 7.07; found: C

8.18, H 2.35, N 7.13.

Red block crystals of **3** and **4** can be obtained respectively in the presence of en and dien when the amount of [Bmmim]Cl was increased to 0.940 g (5 mmol) while maintaining all other parameters unchanged. Elemental analysis, calcd. (%) for C₃₉H₉₉ClMn₂N₁₈Se₂₁Sn₉ (**3**): C 12.69, H 2.70, N 6.83; found: C 12.77, H 2.64, N 6.90 and C₇₀H₁₅₄N₂₄Mn₂Se₃₅Sn₁₅ (**4**): C 14.03, H 2.57, N 5.62; found: C 13.90, H 2.60, N 5.62.

40 X-ray Crystal Structure Determination

Single-crystal X-ray diffraction data were collected on a Xcalibur CCD diffractometer for compounds **1** and **2** at 293(2) K and on a SuperNova CCD diffractometer for compounds **3** and **4** at 100(2) K with MoK α radiation ($\lambda = 0.7107$ Å). The absorption corrections were applied using an analytical technique for **1** and **2**. For **3** and **4**, multi-scan absorption corrections were applied. The structures were solved using direct methods and refined by full-matrix least-squares on F^2 using the SHELX-2013 program.⁵⁶ Anisotropic thermal factors were assigned to most of the non-disordered non-hydrogen atoms, while some disordered non-hydrogen atoms of [Bmmim]⁺ in compound **4** were refined isotropically. The hydrogen atoms bonded to C and N atoms were positioned with idealized geometry, while that in disordered [Bmmim]⁺ of compound **4** were not added. In the four compounds, some restraints (DFIX, SIMU, DELU, FLAT and SADI) were applied to the disordered en, dien, and [Bmmim]⁺ to obtain the chemical-reasonable models and reasonable atomic displacement parameters. The empirical formulae were confirmed by thermogravimetric analysis and element analysis results. Detailed crystallographic data and structure-refinement parameters of compounds **1–4** are summarized in Table 1.

Table 1 Crystal data and structure refinement parameters for compounds **1–4**.

Compound	1	2	3	4
Formula	C ₆ H ₂₄ MnN ₆ Se ₇ Sn ₃	C ₈ H ₂₈ MnN ₆ OSe ₇ Sn ₃	C ₃₉ H ₉₉ ClMn ₂ N ₁₈ Se ₂₁ Sn ₉	C ₇₀ H ₁₅₄ Mn ₂ N ₂₄ Se ₃₅ Sn ₁₅
Mr (g mol ⁻¹)	1144.04	1188.09	3692.06	5985.99
Crystal system	monoclinic	monoclinic	monoclinic	monoclinic
Space group	<i>P</i> 2 ₁ / <i>n</i>	<i>P</i> 2 ₁ / <i>n</i>	<i>P</i> 2 ₁ / <i>c</i>	<i>P</i> 2 ₁ / <i>m</i>
<i>D</i> _{calcd} (g cm ⁻³)	3.005	2.886	2.578	2.639
<i>a</i> (Å)	12.2277(6)	12.3987(5)	19.4488(5)	13.4256(3)
<i>b</i> (Å)	13.1904(5)	13.3150(4)	19.5108(5)	29.9039(10)
<i>c</i> (Å)	15.9272(8)	16.6672(6)	26.6148(7)	19.5845(7)
β (°)	100.174(5)	96.378(4)	109.587(3)	106.643(3)
<i>V</i> (Å ³)	2528.5(2)	2734.54(17)	9514.9(4)	7533.4(4)
<i>Z</i>	4	4	4	2
μ (mm ⁻¹)	13.498	12.489	10.673	11.095
<i>R</i> _{int}	0.0375	0.0269	0.0438	0.0432
Measured refls.	10262	11865	47334	35261
Independent refls.	5174	5747	16760	13520
No. of parameters	208	260	1048	697
<i>R</i> ₁ ^a [<i>I</i> > 2 σ (<i>I</i>)]	0.0381	0.0292	0.0553	0.0780
<i>wR</i> ₂ ^b [<i>I</i> > 2 σ (<i>I</i>)]	0.0766	0.0593	0.1223	0.1562
Goodness of fit	1.026	1.021	1.037	1.025

$$^a R_1 = \sum (F_o - F_c) / \sum F_o, \quad ^b wR_2 = [\sum w(F_o^2 - F_c^2)^2 / \sum w(F_o^2)^2]^{1/2}.$$

Results and discussion

Crystal Structures of **1**, **2**, **3** and **4**

[Mn(en)₃][Sn₃Se₇] (**1**) and [Mn(dien)₂][Sn₃Se₇·H₂O] (**2**). The isostructural compounds **1** and **2** belong to the *P*2₁/*n* space group and feature a two-dimensional lamellar [Sn₃Se₇]_{*n*}²ⁿ⁻ structure that is built up from

[Sn₃Se₁₀] units. The asymmetric unit is composed of a [Mn(amine)_{*x*}]²⁺ complex (amine = en and *x* = 3 for **1**, amine = dien and *x* = 2; for **2**, Fig. 2a) and an anionic [Sn₃Se₇]²⁻ group, in which the Mn²⁺ are coordinated with six N atoms of the chelating amines. As for compound **1**, both *A*($\lambda\lambda\lambda$) and *A*($\delta\delta\delta$) configurations of the [Mn(en)₃]²⁺ are presented as a result of the centrosymmetric nature of the structure, Fig. 2a (left). Correspondingly, the [Mn(dien)₂]²⁺ complexes in **2** also have two

enantiomers, in which the Mn^{2+} is chelated by dien ligands in a *mer*-conformation. As shown in Fig. 2a, the Mn^{2+} ion in **1** is in a distorted octahedral environment with *cis*-N–Mn–N angles varying in $76.1(2)$ – $103.4(2)^\circ$ and *trans*-N–Mn–N angles varying in $160.1(2)$ – $172.6(3)^\circ$ (Fig. 2a, left), and the distances of Mn and N are in the range of $2.254(6)$ – $2.303(7)$ Å. For **2**, the Mn^{2+} ion is in a distorted octahedral environment with *cis*-N–Mn–N angles varying in $74.0(2)$ – $124.9(2)^\circ$ and *trans*-N–Mn–N angles varying in $137.7(3)$ – $153.1(3)^\circ$, and the distances of Mn and N are in the range of $2.282(5)$ – $2.322(5)$ Å (Fig. 2a, right).

Each Sn^{4+} atoms is coordinated to five Se atoms at distances in the range of $2.4885(10)$ – $2.8822(10)$ Å in **1** and $2.5066(7)$ – $2.8298(7)$ Å in **2**. As depicted in Fig. 2b, there exist elliptic six-membered rings in **1** and **2**, regarding the $[\text{Sn}_3\text{Se}_{10}]$ unit as a member. Take the example in **1**, the elliptic six-membered rings in **1** have a major axis about $18.0265(6)$ Å and a minor axis of $12.2577(4)$ Å (Fig. S2, ESI[†]). To satisfy the distortion, the bridging Sn–Se–Sn bond angles for the μ_2 -Se between $[\text{Sn}_3\text{Se}_{10}]$ units are bent between $83.87(3)$ and $96.96(3)^\circ$ in **1**, while those are close to 90° in the regular hexagonal six-membered ring.^{11, 34, 36, 45, 47}

Regarding the $[\text{Sn}_3\text{Se}_{10}]$ semi-cubes as 3-connected nodes, the lamellar $[\text{Sn}_3\text{Se}_7]_n^{2n-}$ network of **1** and **2** shows a topology net of $\{6^3\}$ (Fig. S2, ESI[†]). Similar to that in the reported $[\text{Mn}(\text{PEHA})]\text{Sn}_3\text{Se}_7$ compound,⁴³ the MAC cations are sandwiched in the inter-lamellar space. The distances between the N/C atoms in $[\text{Mn}(\text{en})_3]^{2+}$ and Se^{2-} ions in the layer lie in the range of $3.480(7)$ – $3.949(10)$ Å for **1** and $3.094(8)$ – $3.969(6)$ Å for **2**, respectively, allowing for N–H \cdots Se and C–H \cdots Se hydrogen-bonding interactions between the cations and anionic layers.

illustrating layer stacking and cations filled in the interlayer spaces. H atoms are omitted for clarity.

$(\text{Bmmim})_3[\text{Mn}(\text{en})_3]_2[\text{Sn}_9\text{Se}_{21}]\text{Cl}$ (**3**). Compound **3** belongs to the space group $P2_1/c$, which contains mixed cations of $[\text{Bmmim}]^+$ and MAC. The asymmetric unit of **3** is composed of two $[\text{Mn}(\text{en})_3]^{2+}$ complexes, three $[\text{Bmmim}]^+$ cations, one Cl^- anion and an anionic $[\text{Sn}_9\text{Se}_{21}]^{6-}$ unit. As that in **1**, the Mn^{2+} are coordinated with six N atoms of the en molecules and both the $A(\lambda\lambda\lambda)$ and $A(\delta\delta\delta)$ conformers of the $[\text{Mn}(\text{en})_3]^{2+}$ are presented (Fig. 3a). However, compared to **1**, the elliptic six-membered ring is not presented in the anionic $[\text{Sn}_3\text{Se}_7]_n^{2n-}$ layers. Instead, an eight-membered heart-shaped ring constructed from $[\text{Sn}_3\text{Se}_{10}]$ and $[\text{Sn}_3\text{Se}_9]$ units is found (Fig. 3b). The heart-shaped ring is about $22.1901(7)$ Å in width and $13.4167(3)$ Å in height (Fig. S3, ESI[†]). At the top of the eight-membered ring, the Sn(5) was four-coordinated and the terminal Se(15) atom pointed to the centre of the ring. This dangling selenium atom results in the shortest Sn–Se bond length of $2.4183(15)$ Å in **3**. Compared to that in compounds **1** and **2**, the Sn–Se–Sn bond angles of bridge μ_2 -Se atoms between the $[\text{Sn}_3\text{Se}_{10}]$ units are in a range of $85.68(5)$ and $90.15(5)^\circ$ in this heart-shaped ring, showing a weaker ring tension. In **3**, all the $[\text{Sn}_3\text{Se}_{10}]$ semi-cubes are 3-connected while the $[\text{Sn}_3\text{Se}_9]$ units are 2-connected. From the topology point of view, the $[\text{Sn}_3\text{Se}_7]_n^{2n-}$ layer of **3** still presents a $\{6^3\}$ net considering the 3-connected $[\text{Sn}_3\text{Se}_{10}]$ units as nodes. The adjacent two $[\text{Sn}_3\text{Se}_7]_n^{2n-}$ layers are centrosymmetric and stacked in an A–B–A sequence, forming a channel along the *b*-axis (Fig. 3c). As shown in Fig. 3c, the $[\text{Mn}(\text{en})_3]^{2+}$, $[\text{Bmmim}]^+$ and Cl^- ions reside in the inter-lamellar spaces through hydrogen-bonding interactions among the cations, anions and anionic layers. In addition, the distance between the Se(15) dangling and its nearest neighbouring $[\text{Bmmim}]^+$ cation is $3.8136(13)$ Å, allowing for an anion– π interaction (Fig. S7a and S7c).

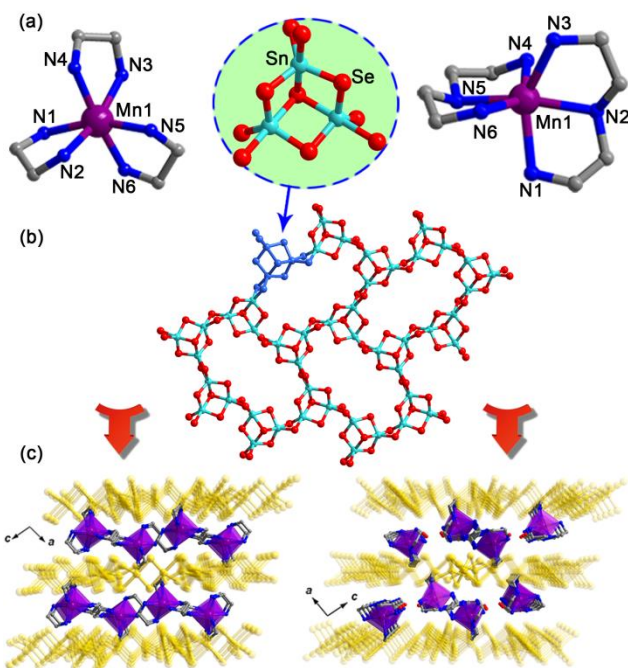


Fig. 2 (a) Structures of the $[\text{Mn}(\text{en})_3]^{2+}$ in **1** (left), $[\text{Sn}_3\text{Se}_{10}]$ unit in **1** and **2** (middle), and $[\text{Mn}(\text{dien})_2]^{2+}$ in **2** (right). (b) Lamellar $[\text{Sn}_3\text{Se}_7]_n^{2n-}$ anion composed of elliptic six-membered rings in **1** and **2**. (c) Side view of **1** and **2** along the *b*-axis

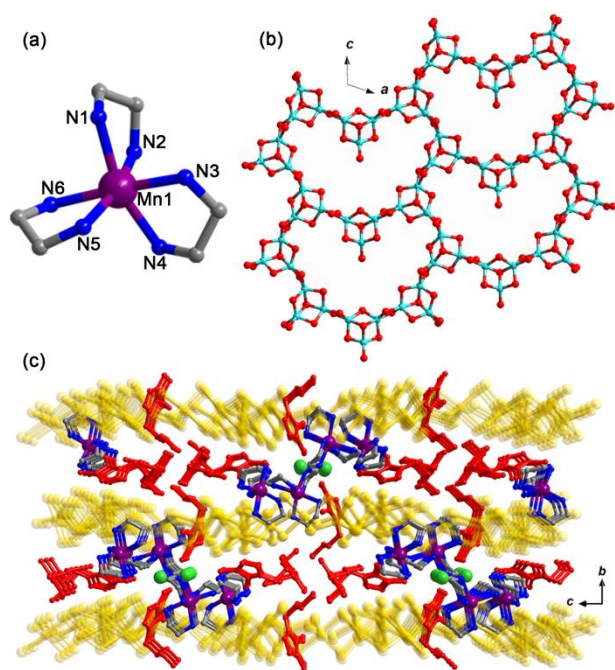


Fig. 3 (a) Structures of the $[\text{Mn}(\text{en})_3]^{2+}$ cation in **3**. (b) Lamellar $[\text{Sn}_3\text{Se}_7]_n^{2n-}$ anion containing eight-membered heart-shaped rings in **3**. (c) Side view of **3** along the a -axis illustrating layer stacking and cations filled in the interlayer spaces and voids. H atoms are omitted for clarity.

$(\text{Bmmim})_6[\text{Mn}(\text{dien})_2]_2[\text{Sn}_{15}\text{Se}_{35}]$ (**4**). Compound **4** belongs to the space group $P2_1/m$. The asymmetric unit of **4** consists of one $[\text{Mn}(\text{dien})_2]^{2+}$ complex, three $[\text{Bmmim}]^+$ cations and two and a half anionic $[\text{Sn}_3\text{Se}_7]^{2-}$ units. Similar to that in **2**, the $[\text{Mn}(\text{dien})_2]^{2+}$ cations in **4** have two enantiomers in which the Mn^{2+} is chelated by dien ligands in *mer*-conformations (Fig. 4a). However, the structure of $[\text{Sn}_3\text{Se}_7]_n^{2n-}$ layer in **4** is different from all those in **1**, **2** and **3**, which consist of both eight-membered heart-shaped rings and compressed six-membered rings (Fig. 4b). The Sn–Se–Sn bond angles of bridging selenium atoms between $[\text{Sn}_3\text{Se}_{10}]$ units range from $85.68(5)$ to $90.15(5)^\circ$, which results in about $22.3040(9)$ Å in width and $13.4820(6)$ Å in height for the heart-shaped ring and $15.5394(5)$ Å in diameter for the six-membered ring (Fig. S4, ESI†). The layer also features a $\{6^3\}$ net topology considering the $[\text{Sn}_3\text{Se}_{10}]$ units as 3-connected nodes. Two adjacent $[\text{Sn}_3\text{Se}_7]_n^{2n-}$ layers are then arranged along the opposite direction and stacked in an A – B – A sequence (Fig. 4c). At the same time, layers A and B offset one another half a unit in adjacent horizon. The layer-by-layer stacking yields channels running down the crystallographic c -axis, with charge-compensating $[\text{Bmmim}]^+$ and $[\text{Mn}(\text{dien})_2]^{2+}$ cations snugly fitting in the inter-lamellar spaces through hydrogen-bonding interactions between the cations and anionic layers (Figs. S7b and S7d, ESI†).

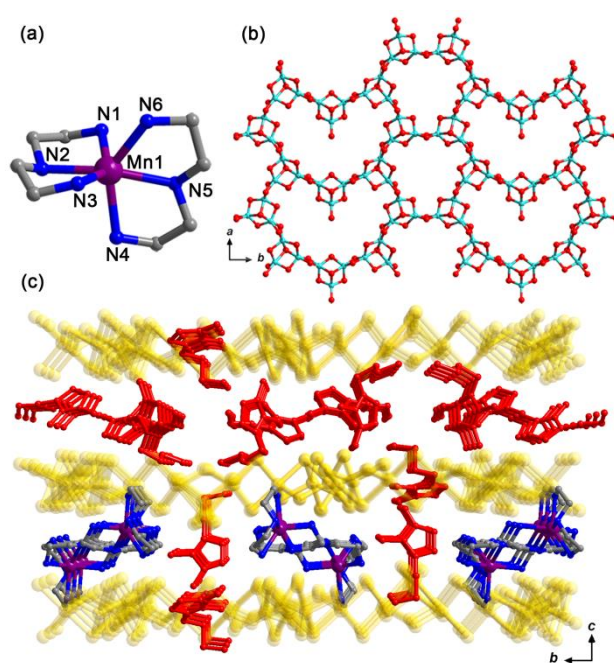


Fig. 4 (a) Structures of the $[\text{Mn}(\text{dien})_2]^{2+}$ cation in **4**. (b) Lamellar $[\text{Sn}_3\text{Se}_7]_n^{2n-}$ anion of eight-membered heart-shaped rings and compressed six-membered rings in **4**. (c) Side view of **4** along the a -axis illustrating layers stacking and cations filled in the interlayer spaces and voids. H atoms are omitted for clarity.

One particular interesting phenomenon is the structural variation of lamellar $[\text{Sn}_3\text{Se}_7]_n^{2n-}$ anions in compounds **1**–**4**. As shown in Fig. 5, the aggregation of the same $[\text{Sn}_3\text{Se}_{10}]$ units via edge-sharing two μ_2 -Se atoms can lead to a single zigzag chain of $[\text{Sn}_3\text{Se}_7]_n^{2n-}$. Then the fusion of $[\text{Sn}_3\text{Se}_7]_n^{2n-}$ single zigzag chains *via* sharing two μ_2 -Se atoms can result in six-membered rings with various degree of distortion. Analogously, the $[\text{Sn}_3\text{Se}_{10}]$ units are firstly connected into $[\text{Sn}_3\text{Se}_7]_n^{2n-}$ single zigzag chain through two μ_2 -Se atoms in **3** and **4**. However, the two symmetric $[\text{Sn}_3\text{Se}_7]_n^{2n-}$ chains are bridged by $[\text{Sn}_3\text{Se}_9]$ units instead of sharing two μ_2 -Se atoms to form an eight-membered heart-shaped ring chain along the crystal c -axis in **3** (Fig. S5a, ESI†) and a -axis in **4** (Fig. S6a, ESI†). Further, the eight-membered heart-shaped ring chains are interconnected through bridging $[\text{Sn}_3\text{Se}_9]$ units to form the lamellar $[\text{Sn}_3\text{Se}_7]_n^{2n-}$ anion in **3** (Fig. S5b, ESI†). Different from the connection in **3**, the parallel eight-membered heart-shaped ring chains in **4** are directly fused into lamellar $[\text{Sn}_3\text{Se}_7]_n^{2n-}$ anion by edge-sharing two μ_2 -Se atoms (Fig. S6†), accompanied by generating a compressed six-membered ring chain between the two eight-membered heart-shaped ring chains. Alternatively, the lamellar $[\text{Sn}_3\text{Se}_7]_n^{2n-}$ anion of **3** can be regarded as interconnection of the single zigzag $[\text{Sn}_3\text{Se}_7]_n^{2n-}$ chains *via* bridging $[\text{Sn}_3\text{Se}_9]$ units.

Cite this: DOI: 10.1039/c0xx00000x

www.rsc.org/xxxxxx

ARTICLE

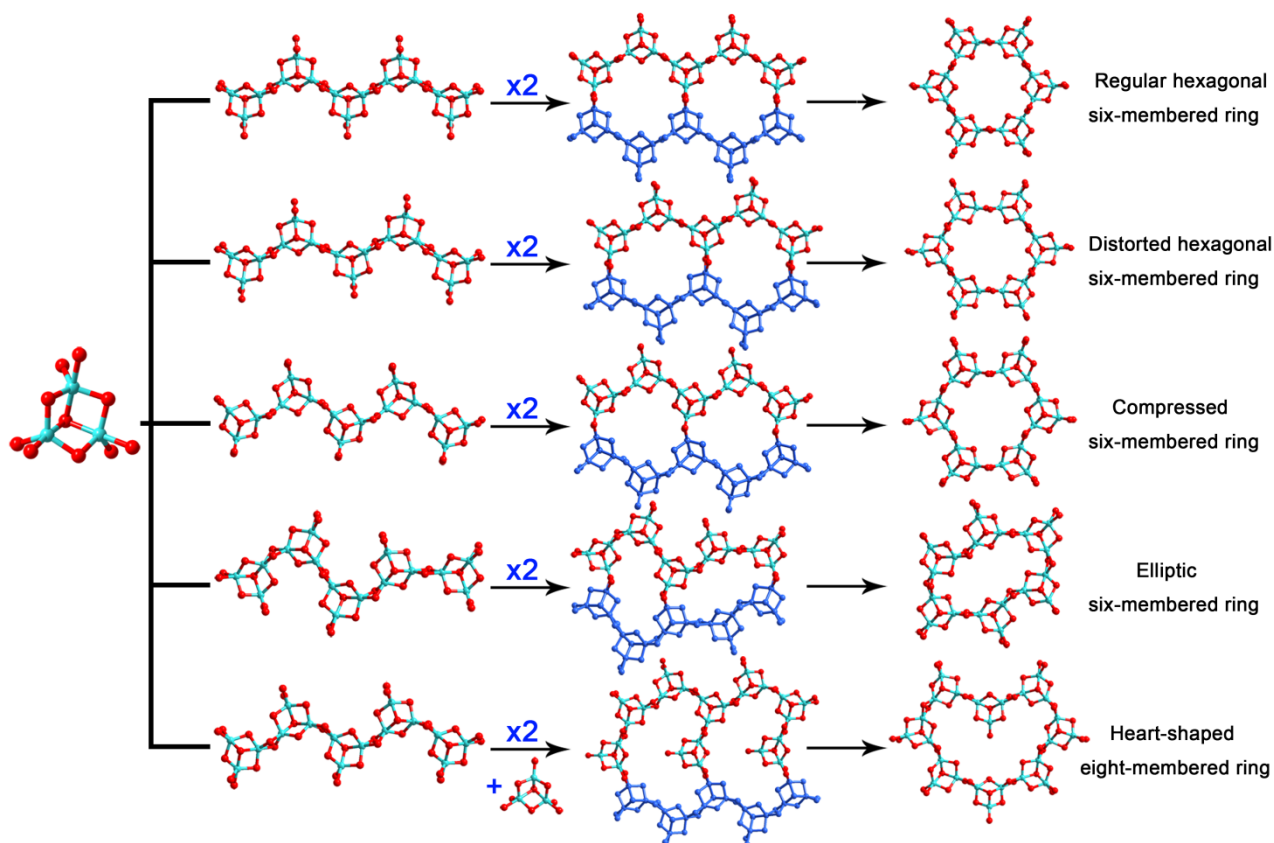


Fig. 5 Structural evolution of the lamellar $[\text{Sn}_3\text{Se}_7]_n^{2n-}$ based on six- or eight-membered rings formed by direct fusion of single $[\text{Sn}_3\text{Se}_7]_n^{2n-}$ zigzag chains or insertion of $[\text{Sn}_3\text{Se}_9]$ units between chains.

A number of compounds containing anionic $[\text{Sn}_3\text{Q}_7]_n^{2n-}$ layers have been synthesized with different cations as SDAs.^{7, 10, 11, 32-51} The counter ions for lamellar $[\text{Sn}_3\text{Se}_7]_n^{2n-}$ anion normally are single alkali ions,¹⁰ organic ammonium,^{11, 36, 40-42} imidazolium^{44, 47} and MAC cations.^{43, 45, 50} As summarized in Table 2, when the organic ammonium cations such as $[\text{enH}]^+$,³² $[\text{Me}_4\text{N}]^+$,^{33, 34} $[\text{Et}_4\text{N}]^+$,³⁹ $[\text{DABCOH}]^+$ ³⁸ or $[1,8\text{-ODA}]^{2+}$ (1,8-octanediamine)⁴² are presented, the regular hexagonal six-membered ring can be found in the lamellar $[\text{Sn}_3\text{Q}_7]_n^{2n-}$; while in the presence of metal-coordinated complex (typically MACs), not only

hexagonal six-membered ring,⁴⁵ but also an elliptic six-membered ring can be established.⁴³ In the ionothermal system, IIs cations can also act as a SDA and result in the hexagonal six-membered ring.⁴⁸ It shall be pointed out that, all the reported lamellar $[\text{Sn}_3\text{Se}_7]_n^{2n-}$ anions feature the varied six-membered rings based on self-condensation of $[\text{Sn}_3\text{Se}_{10}]$ units. It appears that the six-membered ring is the most stable configuration for the $[\text{Sn}_3\text{Q}_7]_n^{2n-}$ layered compounds. Undoubtedly, compounds **3** and **4** represent the first examples of $\text{A}_x\text{Sn}_3\text{Se}_7$ compounds that contain eight-membered ring in the lamellar $[\text{Sn}_3\text{Se}_7]_n^{2n-}$ anions.

Table 2 Different structures of anionic $[\text{Sn}_3\text{Q}_7]_n^{2n-}$ directed by various SDAs.

Structural directing agents	Formula	$[\text{Sn}_3\text{Q}_7]_n^{2n-}$ ring conformation
$[\text{enH}]^+$	$(\text{enH}_2)(\text{en})_{0.5}[\text{Sn}_3\text{Se}_7]^{32}$	regular hexagonal six-membered ring
$[\text{Me}_4\text{N}]^+$	$(\text{Me}_4\text{N})_2[\text{Sn}_3\text{S}_7] \cdot \text{H}_2\text{O},^{34}$ $(\text{Me}_4\text{N})_4[\text{Sn}_6\text{Se}_{14}],^{33}$ $(\text{Me}_4\text{N})_4[\text{Sn}_6\text{Se}_{14}] \cdot 3\text{H}_2\text{O},^{33}$	
$[\text{Me}_3\text{NH}]^+$	$(\text{Me}_3\text{NH})_{2.04}[\text{Sn}_{18}\text{Se}_{42}]_{0.17} \cdot 0.72\text{H}_2\text{O},^{37}$	
$[\text{Et}_4\text{N}]^+$	$(\text{Et}_4\text{N})_2[\text{Sn}_3\text{S}_7],^{39}$	
$[\text{NH}_4]^+$ and $[\text{Et}_4\text{N}]^+$	$(\text{NH}_4)_{0.5}(\text{Et}_4\text{N})_{1.5}[\text{Sn}_3\text{S}_7],^{39}$	
$[\text{trenH}]^+$	$(\text{trenH})_2[\text{Sn}_3\text{S}_7],^{46}$	
$[\text{DABCOH}]^+$	$(\text{DABCOH})_2[\text{Sn}_3\text{S}_7] \cdot \text{H}_2\text{O},^{38}$	
$[1,8\text{-ODA}]^{2+}$	$(1,8\text{-ODA})[\text{Sn}_3\text{Se}_7],^{42}$	
1,3-diaminoethyl-imidazolidone [TETN-CO] ⁺	$(\text{TETN-CO})_2[\text{Sn}_3\text{Se}_7] \cdot \text{H}_2\text{O},^{36}$	
$[\text{Fe}(\text{phen})_3]^{2+}$	$[\text{Fe}(\text{phen})_3][\text{Sn}_3\text{Se}_7] \cdot 1.25\text{H}_2\text{O},^{45}$	

[Prmmim] ⁺	(Prmmim) ₂ [Sn ₃ Se ₇], ⁴⁷	
[Bmmim] ⁺	(Bmmim) ₂ [Sn ₃ Se ₇], ⁴⁷	
[Bmim] ⁺	(Bmim) ₄ [Sn ₆ Se ₁₄], ⁴⁴	
[Bmmim] ⁺	(Bmmim) ₁₆ [Sn ₂₄ Se ₅₆], ⁴⁸	
[Bmmim] ⁺ and [DMMPH] ⁺	(Bmmim) ₃ [DMMPH][Sn ₆ Se ₁₄], ⁴⁸	
[Et ₃ NH] ⁺	(Et ₃ NH) ₂ [Sn ₃ Se ₇] · 0.25H ₂ O, ⁴¹	distorted hexagonal six-membered ring
[Fe(bipy) ₃] ²⁺	[Fe(bipy) ₃] ₂ [Sn ₃ Se ₇] ₂ bipy · 2H ₂ O, ⁵⁰	
[DBNH] ⁺	(DBNH) ₂ [Sn ₃ Se ₇] PEG, ⁵¹	compressed six-membered ring
Cs ⁺	Cs ₂ [Sn ₃ Se ₇], ¹⁰	
[Mn(PEHA)] ²⁺	[Mn(PEHA)][Sn ₃ Se ₇], ⁴³	
[Mn(en) ₃] ²⁺	[Mn(en) ₃][Sn ₃ Se ₇], ⁴	elliptic six-membered ring
[Mn(dien) ₂] ²⁺	[Mn(dien) ₂][Sn ₃ Se ₇] · H ₂ O, ^a	
[Bmmim] ⁺ and [Mn(en) ₃] ²⁺	(Bmmim) ₃ [Mn(en) ₃] ₂ [Sn ₉ Se ₂₁]Cl, ^a	heart-shaped eight-membered ring
[Bmmim] ⁺ and [Mn(dien) ₂] ²⁺	(Bmmim) ₆ [Mn(dien) ₂] ₂ [Sn ₁₅ Se ₃₅], ^a	heart-shaped eight-membered and compressed six-membered ring

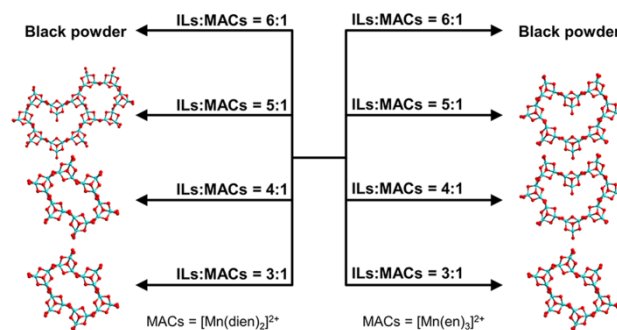
^a The compounds reported in this work.

Structural directing Effects of MAC and IL cations

The synthesis of chalcogenidostannates is sensitive to the nature of SDAs and reaction conditions. Imidazolium-based ILs as well as organic amines have been successfully used in the synthesis of numerous open-framework materials.^{24, 44} Previously, it has been found that the IL and organic amine can cooperatively act as mixed templates in ionothermal syntheses of molecular sieves;²⁶⁻²⁹ the hydrogen bonding interactions between the organic amines and imidazolium cations will facilitate the formation of an aggregated larger cationic complex as a supramolecular inclusion complex or as liquid clathrates.^{27, 57, 58} However, there was no report on the mixed cations containing MACs and imidazolium cations. For this reason, the structural directing effect of IL cations and MACs in ionothermal system attracted our attention. In this work, a series of reactions with a variety molar ratios of ILs over MACs has been carried out and four selenidostannate compounds with different lamellar [Sn₃Se₇]_n²ⁿ⁻ configurations were obtained *via* carefully regulating the ratio of ILs and MACs. The relationship between structural variation and the ratio of ILs over MACs is sketchily drawn in Scheme 1. When the amounts of IL cations were in large excess over that of MACs cations (*e.g.* in a mole ratios beyond 6:1), a mixture of unknown black powder was obtained. When the amounts of ionic liquids were decreased ([Bmmim]Cl:MnCl₂ = 3:1, molar ratio) while the other reaction conditions remained unchanged, the MACs-Sn₃Se₇ species could be obtained. Interestingly, when the IL: MAC ratios were increased to 4:1 and 5:1 for en and dien, respectively, the two cations ([Bmmim]⁺ and MAC) could simultaneously enter the resulting structure and the eight-membered heart-shaped ring configuration in [Sn₃Se₇]_n²ⁿ⁻ was found for the first time.

In addition, comparing the three MAC-directed lamellar A_xSn₃Se₇ compounds (**1**, **2** and [Mn(PEHA)]Sn₃Se₇), it is clearly found that MACs with different organic amines show similar structural directing effect when they act as a single SDA, but the final products were different while they simultaneously worked with identical IL cation (here, [Bmmim]⁺). The structural evolution from compounds **1** and **2** containing single MAC cations to compounds **3** and **4** containing mixed cations clearly demonstrated that there was a competitive and synergistic effect of various SDAs in ionothermal syntheses of lamellar selenidostannates. As discussed above, the different MACs in the structures interact with the [Sn₃Se₇]_n²ⁿ⁻ layers through hydrogen bonding. The main reason for the structural variation between **3**

and **4** may be due to the synergistic effects of [Bmmim]⁺ cations and MACs, which provided hydrogen bonds and anion-π interactions with [Sn₃Se₇]_n²ⁿ⁻ layers and MACs cations.



Scheme 1 Different products controlled by varying the [Bmmim]⁺:MAC ratios under the similar reaction conditions.

Powder X-ray Diffraction Analyses and Thermal Properties

All the crystals were manual selected and used for further characterizations. The phase purity of the products was confirmed by PXRD analysis and EA analyses. As shown in Fig. 6, the experimental PXRD patterns of the title compounds are in accordance with the corresponding simulated PXRD patterns from single-crystal X-ray structures, demonstrating the phase purity of the four compounds. Preferred orientation was evidenced due to the lamellar nature of the title compounds; for instance, the intensive (002) and (004) reflections in the experimental PXRD pattern of **4** illustrated in Fig. 6.

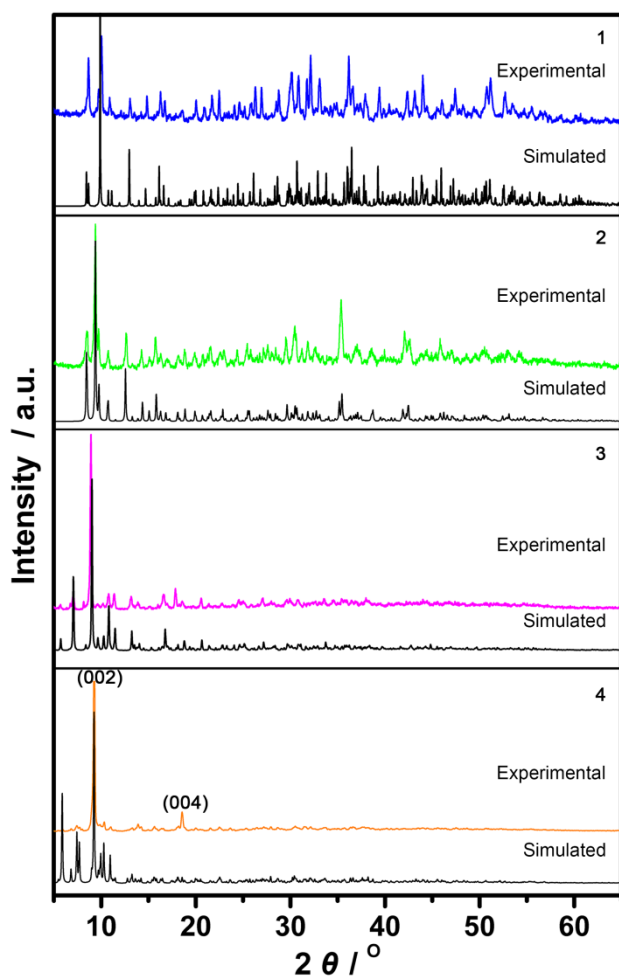


Fig. 6 The experimental and simulated PXRD patterns of 1–4.

Thermogravimetric analyses (TGA) were performed on pure polycrystalline samples of 1–4 in a N_2 atmosphere from 30 to 550 $^{\circ}C$. As shown in Fig. 7, all the weight losses are in correspondence with the losses of organic components and H_2Se molecules.²⁴ The post-TGA residues for the four compounds were identified as the mixture of $MnSe$, $SnSe$ and/or $SnSe_2$ (Figs. S8–S11[†]) by PXRD.

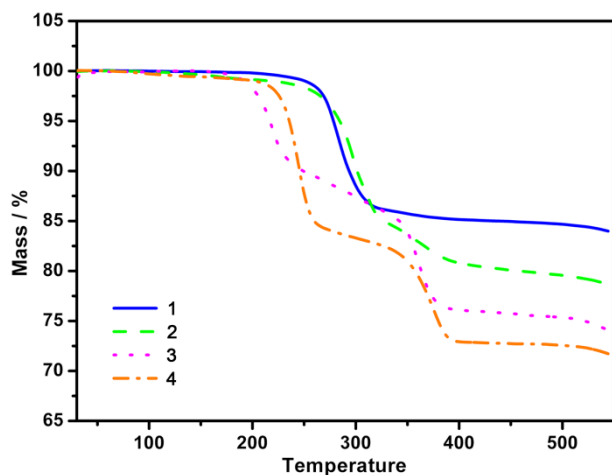


Fig. 7 TG curves of 1–4 at a heating rate of 10 $K\ min^{-1}$ in a N_2 atmosphere from 30 to 550 $^{\circ}C$.

Optical Properties

Solid state absorption spectra of compounds 1–4 at room temperature are plotted in Fig. 8. The spectra indicate a sharp absorption edge at about 1.99 eV for 1, 2.04 eV for 2, 1.96 eV for 3 and 1.93 eV for 4, respectively, which are consistent with their colours and all are located in the visible region. Compared to that of $(Bmmim)_2Sn_3Se_7$, which has an absorption edge at about 2.2 eV,⁴⁷ it can be found that the addition of MACs cations into the structure results in a red shift of the absorption edge.

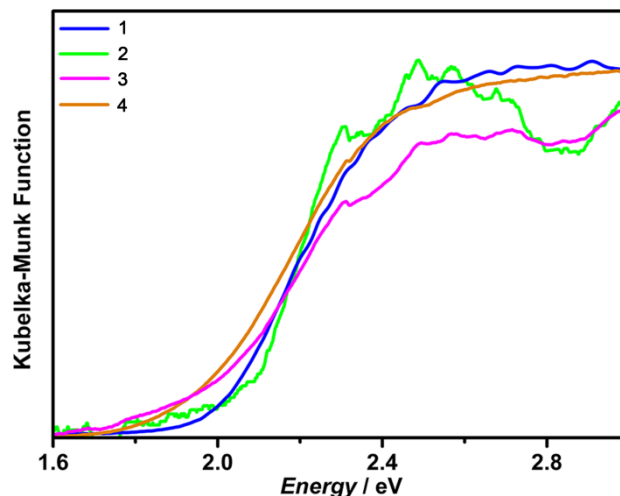


Fig. 8 Solid state optical absorption spectra of compounds 1–4.

Conclusions

In summary, by using the metal-amine complexes (MACs) and/or ionic liquid $(Bmmim)Cl$ as structural directing agents, four new selenidostannate compounds with various lamellar $[Sn_3Se_7]_n^{2n-}$ anion were prepared. It is noted that the eight-membered heart-shaped ring in the family of lamellar $[Sn_3Se_7]_n^{2n-}$ anion was discovered for the first time. The compounds 3 and 4 represent the first examples of chalcogenidometallates simultaneously contain MACs and imidazolium cations. The structural variation from 1 to 4 clearly demonstrates the competitive and synergistic effect of MACs and IL cations in directing selenidostannates. The synthetic approach via varying the ratio of MAC and IL cation as solvent and structural directing agents shall be attractive in the synthesis of novel chalcogenidometallates.

Acknowledgement

This work was supported by the 973 program (No. 2014CB845603) and the NNSF of China (No. 21371001).

Notes and references

- ^a State Key Laboratory of Structural Chemistry, Fujian Institute of Research on the Structure of Matter, Chinese Academy of Sciences, Fuzhou, Fujian, 350002, People's Republic of China. Fax: +86 0591 63173146; Tel: +86 0591 63173146; E-mail: jrli@fjirsm.ac.cn
- ^b University of Chinese Academy of Sciences, Beijing, 100049, People's Republic of China.
- ^c College of Chemistry and Chemical Engineering, Xinyang Normal University, Xinyang 464000, China.

- † Electronic Supplementary Information (ESI) available: [Crystallographic data for **1**, **2**, **3** and **4** in CIF format, additional structural figures, PXRD patterns for TG residues and EDX spectra. CCDC reference numbers 1042762-1042765]. See DOI: 10.1039/b000000x/
1. J. A. Rogers, M. G. Lagally and R. G. Nuzzo, *Nature*, 2011, **477**, 45-53.
 2. Q. Tian, G. Wang, W. Zhao, Y. Chen, Y. Yang, L. Huang and D. Pan, *Chem. Mater.*, 2014, **26**, 3098-3103.
 3. M. L. Feng, D. N. Kong, Z. L. Xie and X. Y. Huang, *Angew. Chem., Int. Ed.*, 2008, **47**, 8623-8626.
 4. N. F. Zheng, X. H. Bu and P. Y. Feng, *Nature*, 2003, **426**, 428-432.
 5. N. Zheng, X. H. Bu, H. Vu and P. Y. Feng, *Angew. Chem., Int. Ed.*, 2005, **44**, 5299-5303.
 6. Z. Y. Zhang, J. Zhang, T. Wu, X. H. Bu and P. Y. Feng, *J. Am. Chem. Soc.*, 2008, **130**, 15238-15239.
 7. T. Jiang, A. J. Lough, G. A. Ozin, D. Young and R. L. Bedard, *Chem. Mater.*, 1995, **7**, 245-248.
 8. T. Jiang, A. Lough, G. A. Ozin and R. L. Bedard, *J. Mater. Chem.*, 1998, **8**, 733-741.
 9. T. Jiang and G. A. Ozin, *J. Mater. Chem.*, 1998, **8**, 1099-1108.
 10. W. S. Sheldrick and H. G. Braunbeck, *Z. Naturforsch., B: Chem. Sci.*, 1990, **45**, 1643-1646.
 11. H. Ahari, A. Lough, S. Petrov, G. A. Ozin and R. L. Bedard, *J. Mater. Chem.*, 1999, **9**, 1263-1274.
 12. W. S. Sheldrick and M. Wachhold, *Coord. Chem. Rev.*, 1998, **176**, 211-322.
 13. W. S. Sheldrick, *Dalton Trans.*, 2000, 3041-3052.
 14. J. Zhou, J. Dai, G. Q. Bian and C. Y. Li, *Coord. Chem. Rev.*, 2009, **253**, 1221-1247.
 15. M. L. Feng, P. X. Li, K. Z. Du and X. Y. Huang, *Eur. J. Inorg. Chem.*, 2011, 3881-3885.
 16. J. Zhou, X. H. Yin and F. Zhang, *Inorg. Chem.*, 2010, **49**, 9671-9676.
 17. J. Zhou, L. An and F. Zhang, *Inorg. Chem.*, 2011, **50**, 415-417.
 18. K. Y. Wang, D. Ye, L. J. Zhou, M. L. Feng and X. Y. Huang, *Dalton Trans.*, 2013, **42**, 5430-5437.
 19. R. D. Rogers and K. R. Seddon, *Science*, 2003, **302**, 792-793.
 20. R. E. Morris, *Chem. Commun.*, 2009, 2990-2998.
 21. T. Welton, *Chem. Rev.*, 1999, **99**, 2071-2083.
 22. S. A. Forsyth, J. M. Pringle and D. R. MacFarlane, *Aust. J. Chem.*, 2004, **57**, 113-119.
 23. L. Wang, Y. P. Xu, Y. Wei, J. C. Duan, A. B. Chen, B. C. Wang, H. J. Ma, Z. J. Tian and L. W. Lin, *J. Am. Chem. Soc.*, 2006, **128**, 7432-7433.
 24. J. R. Li, Z. L. Xie, X. W. He, L. H. Li and X. Y. Huang, *Angew. Chem., Int. Ed.*, 2011, **50**, 11395-11399.
 25. Y. Lin, W. Massa and S. Dehnen, *J. Am. Chem. Soc.*, 2012, **134**, 4497-4500.
 26. H. Z. Xing, J. Y. Li, W. F. Yan, P. Chen, Z. Jin, J. H. Yu, S. Dai and R. R. Xu, *Chem. Mater.*, 2008, **20**, 4179-4181.
 27. R. Xu, W. Zhang, J. Guan, Y. Xu, L. Wang, H. Ma, Z. Tian, X. Han, L. Lin and X. Bao, *Chem. Eur. J.*, 2009, **15**, 5348-5354.
 28. R. Pei, Y. Wei, K. Li, G. Wen, R. Xu, Y. Xu, L. Wang, H. Ma, B. Wang, Z. Tian, W. Zhang and L. Lin, *Dalton Trans.*, 2010, **39**, 1441-1443.
 29. Y. Wei, B. Marler, L. Zhang, Z. Tian, H. Graetsch and H. Gies, *Dalton Trans.*, 2012, **41**, 12408-12415.
 30. J. Li, B. Marler, H. Kessler, M. Soulard and S. Kallus, *Inorg. Chem.*, 1997, **36**, 4697-4701.
 31. A. Fehlker and R. Blachnik, *Z. Anorg. Allg. Chem.*, 2001, **627**, 411-418.
 32. W. S. Sheldrick and H. G. Braunbeck, *Z. Anorg. Allg. Chem.*, 1993, **619**, 1300-1306.
 33. T. Jiang, G. A. Ozin and R. L. Bedard, *Adv. Mater.*, 1994, **6**, 860-865.
 34. J. B. Parise, Y. Ko, J. Rijssenbeek, D. M. Nellis, K. Tan and S. Koch, *J. Chem. Soc., Chem. Commun.*, 1994, 527.
 35. Y. Ko, K. Tan, D. M. Nellis, S. Koch and J. B. Parise, *J. Solid State Chem.*, 1995, **114**, 506-511.
 36. J. B. Parise, Y. Ko, K. Tan, D. M. Nellis and S. Koch, *J. Solid State Chem.*, 1995, **117**, 219-228.
 37. K. Tan, Y. Ko and J. B. Parise, *Acta Crystallogr. C*, 1995, **51**, 398-401.
 38. T. Jiang, A. Lough and G. A. Ozin, *Adv. Mater.*, 1998, **10**, 42-46.
 39. T. Jiang, A. Lough, G. A. Ozin, R. L. Bedard and R. Broach, *J. Mater. Chem.*, 1998, **8**, 721-732.
 40. A. Loose and W. S. Sheldrick, *Z. Anorg. Allg. Chem.*, 1999, **625**, 233-240.
 41. A. Fehlker and R. Blachnik, *Z. Anorg. Allg. Chem.*, 2001, **627**, 1128-1134.
 42. S. Lu, Y. Ke, J. Li, S. Zhou, X. Wu and W. Du, *Struct. Chem.*, 2003, **14**, 637-642.
 43. G. H. Xu, C. Wang and P. Guo, *Acta Crystallogr. C*, 2009, **65**, M171-M173.
 44. Y. M. Lin and S. Dehnen, *Inorg. Chem.*, 2011, **50**, 7913-7915.
 45. G. N. Liu, G. C. Guo, M. J. Zhang, J. S. Guo, H. Y. Zeng and J. S. Huang, *Inorg. Chem.*, 2011, **50**, 9660-9669.
 46. N. Pienack, D. Schinkel, A. Puls, M.-E. Ordolff, H. Lühmann, C. Näher and W. Bensch, *Z. Naturforsch., B: Chem. Sci.*, 2012, **67b**, 1098-1106.
 47. J. R. Li, W. W. Xiong, Z. L. Xie, C. F. Du, G. D. Zou and X. Y. Huang, *Chem. Commun.*, 2013, **49**, 181-183.
 48. Y. M. Lin, D. W. Xie, W. Massa, L. Mayrhofer, S. Lippert, B. Ewers, A. Chernikov, M. Koch and S. Dehnen, *Chem. Eur. J.*, 2013, **19**, 8806-8813.
 49. Q. Lin, X. Bu and P. Feng, *Chem. Commun.*, 2014, **50**, 4044-4046.
 50. C. Tang, F. Wang, J. Lu, D. Jia, W. Jiang and Y. Zhang, *Inorg. Chem.*, 2014, **53**, 9267-9273.
 51. W. W. Xiong, J. Miao, K. Ye, Y. Wang, B. Liu and Q. Zhang, *Angew. Chem., Int. Ed.*, 2014.
 52. C.-W. Park, M. A. Pell and J. A. Ibers, *Inorg. Chem.*, 1996, **35**, 4555-4558.
 53. J. Zhou, G. Q. Bian, J. Dai, Y. Zhang, A. B. Tang and Q. Y. Zhu, *Inorg. Chem.*, 2007, **46**, 1541-1543.
 54. W. M. Wendlandt and H. G. Hecht, Interscience, New York, 1966.
 55. J. Zhang, J. Xi and Z. Ji, *J. Mater. Chem.*, 2012, **22**, 17700.
 56. G. M. Sheldrick, *Acta Crystallogr. A*, 2008, **64**, 112-122.
 57. J. D. Holbrey, W. M. Reichert, M. Nieuwenhuizen, O. Sheppard, C. Hardacre and R. D. Rogers, *Chem. Commun.*, 2003, 476-477.
 58. L. Leclercq and A. R. Schmitzer, *Supramol. Chem.*, 2009, **21**, 245-263.